2010

Membrane Anchor R9AP Potentiates GTPase-accelerating Protein Activity of RGS11·$G\beta_5$ Complex and Accelerates Inactivation of the mGluR6-G_0 Signaling

Ikuro Masuho

Jeremy Celver
University of Rhode Island

See next page for additional authors

Citation/Publisher Attribution

Masuho, I., Celver, J., Kovoor, A., & Martemyanov, K. A. (2010). Membrane Anchor R9AP Potentiates GTPase-accelerating Protein Activity of RGS11·$G\beta_5$ Complex and Accelerates Inactivation of the mGluR6-G_0 Signaling. *Journal of Biological Chemistry, 285*, 4781-4787. doi: 10.1074/jbc.M109.058511
Available at: http://dx.doi.org/10.1074/jbc.M109.058511

THE JOURNAL OF BIOLOGICAL CHEMISTRY VOL. 285, NO. 7, pp. 4781–4787, February 12, 2010

Membrane Anchor R9AP Potentiates GTPase-accelerating Protein Activity of RGS11·Gβ_5 Complex and Accelerates Inactivation of the mGluR6-G$_o$ Signaling*[S]

Received for publication, August 24, 2009, and in revised form, October 22, 2009 Published, JBC Papers in Press, December 11, 2009, DOI 10.1074/jbc.M109.058511

Ikuo Masuho[‡], Jeremy Celver[§], Abraham Kovoor[§1], and Kirill A. Martemyanov[‡2]

From the [‡]Department of Pharmacology, University of Minnesota, Minneapolis, Minnesota 55455 and the [§]Department of Biomedical and Pharmaceutical Sciences, University of Rhode Island, Kingston, Rhode Island 02881

The R7 subfamily of RGS proteins critically regulates neuronal G protein-signaling pathways that are essential for vision, nociception, motor coordination, and reward processing. A member of the R7 RGS family, RGS11, is a GTPase-accelerating protein specifically expressed in retinal ON-bipolar cells where it forms complexes with the atypical G protein β subunit, Gβ_5, and transmembrane protein R9AP. Association with R9AP has been shown to be critical for the proteolytic stability of the complex in the retina. In this study we report that R9AP can in addition stimulate the GTPase-accelerating protein activity of the RGS11·Gβ_5 complex at Gα_o. Single turnover GTPase assays reveal that R9AP co-localizes RGS11·Gβ_5 and Gα_o on the membrane and allosterically potentiates the GTPase-accelerating function of RGS11·Gβ_5. Reconstitution of mGluR6-Gα_o signaling in *Xenopus* oocytes indicates that RGS11·Gβ_5-mediated GTPase acceleration in this system requires co-expression of R9AP. The results provide new insight into the regulation of mGluR6-Gα_o signaling by the RGS11·Gβ_5·R9AP complex and establish R9AP as a general GTPase-accelerating protein activity regulator of R7 RGS complexes.

Regulators of G protein signaling (RGS)[3] are ubiquitous signaling molecules that critically shape cellular responses mediated by G protein-coupled receptor (GPCR) pathways (1). Most RGS proteins act by stimulating the rate of the GTP hydrolysis of the α subunits of G proteins (Gα), thus speeding up their inactivation and limiting the duration of GPCR signaling (2). R7 subfamily of RGS proteins plays a central role in regulating fundamental neuronal functions including vision, nociception, reward processing, and motor control (3–6). The subfamily consists of four homologous proteins, RGS6, RGS7, RGS9, and RGS11, that are enriched in the nervous system and share a common multidomain architecture that, in addition to the catalytic RGS domain, includes an N-terminal DEP/DHEX (Dishevelled, EGL-10, Pleckstrin/DEP helical extension) module and a GGL (G protein γ subunit-like) domain (7).

In vivo, R7 RGS proteins are found in complexes with two types of proteins that are becoming increasingly accepted as their subunits. The GGL forms a complex with the atypical G protein β subunit, Gβ_5 (8). The DEP/DHEX module binds to either R7BP (R7 family binding protein) or R9AP (RGS9 anchor protein) (9, 10), a two-member family of small SNARE (soluble *N*-ethylmaleimide factor attachment protein receptor)-like proteins. Association with both Gβ_5 (11, 12) and R7BP/R9AP (13–15) protects complexes from proteolytic degradation and, thus, plays an important role in regulating the expression levels of the R7 RGS proteins. In addition, membrane proteins R9AP and R7BP can localize R7 RGS proteins to cell membranes in transfected cells and native neurons (16–18). Finally, R9AP has been shown to enhance the GTPase-accelerating protein (GAP) activity of RGS9-1 toward transducin, suggesting that membrane anchors also play a role in regulation of R7 RGS activity (10, 19–21). However, what remains unclear is (i) if the potentiation of the GAP activity of R7 RGS members is a universal mode of action for the R9AP or R7BP membrane anchors, (ii) whether R9AP can stimulate GAP activity of R7 RGS proteins at G proteins other than transducin, and (iii) whether the stimulation of GAP function results simply from the effect of concentrating R7 protein at the cell membrane or from a more complicated mechanism, requiring additional allosteric contributions.

Previously, R9AP has been shown to be expressed in retinal photoreceptor cells where it regulates the photoreceptor-specific R7 RGS protein complex, RGS9-1·Gβ_5 (4, 14, 18). Recently, we have discovered R9AP in a novel heterotrimeric complex with another R7 RGS protein, RGS11 (23). The R9AP·RGS11·Gβ_5 complex is exclusively expressed in retinal ON-bipolar neurons which relay the light-elicited signals from the photoreceptors to ganglion cells in the circuit that connects the photoreceptors to the brain (23–26). The complex is targeted to the dendritic tips of the ON-bipolar neurons via the association with the mGluR6 (23), a Gα_o-coupled GPCR, that responds to light-induced changes in glutamate release from the photoreceptor terminals (for review, see Ref. 27). Studies

* This work was supported, in whole or in part, by National Institutes of Health Grants EY018139 (to K. A. M.), DA026405 (to K. A. M.), and R41MH078570 (to J. C. and A. K.). This work was also supported by a McKnight Land Grant award (to K. A. M.).

[S] The on-line version of this article (available at http://www.jbc.org) contains supplemental Figs. 1–5.

[1] To whom correspondence may be addressed: 57 Fogarty Hall, 41 Lower College Rd., Kingston, RI 02881. Fax: 401-874-5787; E-mail: abekovoor@uri.edu.

[2] To whom correspondence may be addressed: 6-120 Jackson Hall, 321 Church St. S.E., Minneapolis, MN 55455. Fax: 612-625-8408; E-mail: martemyanov@umn.edu.

[3] The abbreviations used are: RGS, regulators of G protein signaling; GPCR, G protein-coupled receptor; GAP, GTPase-accelerating protein; GIRK, G protein inwardly rectifying potassium; uROS, rod outer segments treated by urea; PTX, pertussis toxin; Sup, supernatant; Ppt, pellet; GST, glutathione *S*-transferase; CHAPS, 3-[(3-cholamidopropyl)dimethylammonio]-1-propanesulfonic acid.

with knock-out mice suggest that RGS11 is involved in determining the kinetics of the overall synaptic transmission between photoreceptor and bipolar neurons (24) and that all subunits of the R9AP·RGS11·Gβ_5 complex are indispensable for its appropriate localization and expression in the bipolar neurons (23).

In this study we have investigated the impact of R9AP on the functional activity of the RGS11·Gβ_5 complex. We show that recruitment of RGS11·Gβ_5 to the plasma membrane by R9AP results in a substantial increase in the GAP activity of the complex toward lipid-modified but not soluble Gα_o. We reconstituted the mGluR6-G_o-RGS11 signaling cascade in *Xenopus* oocytes and utilized the acceleration of the deactivation kinetics of co-expressed G protein inwardly rectifying potassium (GIRK) channels as a measure of RGS11 GAP function. Activity of RGS11 in this assay system was discerned only when R9AP was co-expressed. These results establish that membrane anchoring by R9AP is a general mechanism for regulating activity of R7 RGS complexes and, in the case of RGS11, is an essential prerequisite for controlling Gα_o signaling through mGluR6.

EXPERIMENTAL PROCEDURES

Antibodies—The generation of rabbit anti-R9AP (against amino-acids 144–223) (28), sheep anti-RGS11 CT (29), and rabbit anti-RGS11 CT (30) antibodies has been described previously. Mouse monoclonal anti-His_6 (Clontech), rabbit anti-glutathione *S*-transferase (GST; Z-5; Santa Cruz Biotechnology), and rabbit anti-Gα_o (K-20; Santa Cruz Biotechnology) antibodies were purchased.

Protein Purification—Purification of RGS9-1·Gβ_5L (31), GST-R9APΔTM (19), and soluble Gα_o expressed in *Escherichia coli* (32) was conducted as described previously. For the purification of the RGS11·Gβ_5S complex, Sf9 cells from 1 liter of Sf9 culture were harvested 48 h after co-infection with amplified recombinant baculoviruses encoding His-tagged RGS11 and Gβ_5S, resuspended in 40 ml of lysis buffer (20 mM HEPES, pH 8.0, 100 mM NaCl, 10 mM imidazole, 5% glycerol, 10 mM β-mercaptoethanol), and then lysed by sonication. All purification steps were conducted at 4 °C using ice-cold buffers supplemented with protease inhibitors. Lysates were centrifuged at 30,000 × *g* for 30 min, after which the supernatants were diluted with 160 ml of lysis buffer and loaded onto a HisTrap HP 1 ml column (GE Healthcare) equilibrated with lysis buffer. The column was washed with 10 volumes of wash buffer (20 mM HEPES, pH 8.0, 400 mM NaCl, 20 mM imidazole, 5% glycerol, 10 mM β-mercaptoethanol), and the His-tagged RGS11·Gβ_5S complexes were eluted by generating increasing imidazole concentrations with wash buffer mixed with elution buffer (20 mM HEPES, pH 8.0, 400 mM NaCl, 300 mM imidazole, 10 mM β-mercaptoethanol, 5% glycerol). Peak fractions containing RGS11·Gβ_5S complexes were pooled, and a buffer exchange was performed using a Zeba Desalt Spin Column (Thermo Fisher Scientific) equilibrated with storage buffer (20 mM Tris-HCl, pH 7.8, 300 mM NaCl, 10% glycerol).

Purification of G_o from Sf9 cells was conducted as described previously with modifications (33). Briefly, Sf9 cells from 1 liter of culture were harvested 48 h after infection with recombinant baculoviruses encoding rat Gα_{oA}, Gβ_1, and His-tagged Gγ_2, resuspended in lysis buffer (20 mM HEPES, pH 8.0, 500 mM NaCl, 2 mM $MgCl_2$, 10 μM GDP, 20 mM imidazole, 10 mM β-mercaptoethanol), and then lysed by sonication. Lysates were centrifuged at 30,000 × *g* for 30 min, and the resultant pellets were washed with wash buffer (lysis buffer containing 1 mM $MgCl_2$). The pellets were resuspended in wash buffer. $C_{12}E_{10}$ detergent was added to a final concentration of 1% (w/v), and the mixture was stirred for 1 h before centrifugation at 30,000 × *g* for 30 min. The supernatants were loaded onto a 1-ml nickel-Sepharose High Performance (GE Healthcare) equilibrated with buffer A (wash buffer containing 0.2% (w/v) $C_{12}E_{10}$). The beads were washed with 25 volumes of buffer A and further washed with 10 volumes of buffer B (wash buffer containing 0.2% (w/v) CHAPS and 1 mM β-mercaptoethanol). The G_o was eluted with elution buffer (wash buffer containing 500 mM imidazole, 0.7% (w/v) CHAPS, and 1 mM β-mercaptoethanol). Fractions containing G_o were pooled and concentrated to ~10 mg/ml. Finally, buffer was exchanged to storage buffer (20 mM HEPES, pH 8.0, 300 mM NaCl, 1 mM $MgCl_2$, 1 μM GDP, 0.7% CHAPS, 10% glycerol, 1 mM β-mercaptoethanol) by a Zeba Desalt Spin Column (Thermo Scientific).

Membrane Preparations—Rod outer segments treated by urea (uROS) and V8-uROS membranes were prepared as described previously with minor modifications (20). For the preparation of insect cell membranes, Sf9 cells and Sf9 cells infected with amplified recombinant baculoviruses encoding R9AP were sonicated in membrane preparation buffer (10 mM Tris-HCl, pH 7.8, 100 mM NaCl, and 8 mM $MgCl_2$), and crude cellular debris was sedimented at 1200 × *g* for 5 min. The membranes were then sedimented at 30,000 × *g* for 30 min and washed 3 times with wash buffer (10 mM Tris-HCl, pH 7.8, 500 mM NaCl, and 8 mM $MgCl_2$). The membranes were stored at −80 °C in membrane preparation buffer containing 10% glycerol. All steps were conducted at 4 °C using ice-cold buffers supplemented with protease inhibitors. Total protein concentration was determined by Bradford assay.

Single Turnover GTPase Assay—Single turnover GTPase assays were conducted as described previously (34). Assays were performed at room temperature in GTPase buffer (10 mM Tris-HCl, pH 7.8, 250 mM NaCl, 8 mM $MgCl_2$, and 1 mM dithiothreitol). Illuminated uROS or V8-uROS were used as the source of photoexcited rhodopsin required for G protein activation. The reaction was started by the addition of 10 μl of 200 nM [γ-^{32}P]GTP (~10^5 cpm/sample) to 20 μl of uROS or V8-uROS membranes reconstituted with appropriate proteins and membranes from Sf9 cells. Final concentrations in the reactions were 20 μM rhodopsin, 1.0 μM G$\alpha_o\beta_1\gamma_2$ heterotrimer purified from Sf9 cells or 1.0 μM Gα_o (*E. coli*) reconstituted with 1.0 μM $\beta_1\gamma_1$ complex, 180 nM RGS11·Gβ_5, 0.68 μM GST, 0.68 μM GST-R9APΔTM, and 0.5 mg/ml Sf9 or R9AP-Sf9 membrane preparations unless otherwise mentioned. The reaction was stopped by the addition of 100 μl of 6% perchloric acid. Phosphate released from hydrolyzed GTP was determined by activated charcoal assay (35). Because high efficiency interactions between RGS9-1·Gβ_5L and Gα_o require the presence of the γ subunit of phosphodiesterase, type 6 (PDEγ) (32, 36), we conducted the assay in the presence of 1.0 μM PDEγ. The relative amount of RGS9-1 and RGS11 used in the assays was deter-

mined by Western blotting. Control experiments were performed to ensure that single turnover conditions are maintained and that GDP/GTP exchange does not limit the GTP hydrolysis (see Refs. 34 and 35 for a description of the criteria and supplemental Fig. 1 for results).

Membrane Binding Assay—A membrane binding assay was performed as described previously (20). Briefly, all experiments were conducted in GTPase buffer at 4 °C. Recombinant RGS9-1·Gβ_5L or RGS11·Gβ_5S was mixed with membranes in the volume of 100 μl, and the mixture was loaded on a 50-μl cushion containing 10% sucrose in GTPase buffer. The mixture was sedimented at 120,000 × *g* for 15 min in a TL-100 ultracentrifuge (Beckman Instruments). Supernatants were collected, whereas the sucrose cushions were discarded. The pellet was washed once by GTPase buffer containing 1 M NaCl to reduce nonspecific protein binding and once by GTPase buffer and then resuspended in 100 μl of GTPase buffer. In some experiments, when indicated, the wash step was skipped. Input, resuspended Ppt and Sup fractions were subjected to SDS-PAGE on 12.5% polyacrylamide gels, and the contents of RGS11·Gβ_5S, RGS9-1·Gβ_5L, R9AP, and Gα_o in each sample were determined by Western blot. For the membrane binding assays of Gα_o, 10 mM NaF, 20 μM $AlCl_3$, and 10 μM GDP were added into all buffers to activate Gα_o and release from G$\beta\gamma$ so that we can test membrane binding activity of free Gα subunits. The final concentrations in the binding reactions were 50 nM RGS9-1·Gβ_5L complexes, 27 nM RGS11·Gβ_5S, 1.0 μM GST, 1.0 μM GST-R9APΔTM, 0.5 mg/ml Sf9 membranes, 0.5 mg/ml R9AP membranes, and uROS and V8-uROS containing 20 μM rhodopsin.

Oocyte Expression Assays—Published methods were used for these studies (37). cRNA was synthesized *in vitro* from plasmids containing the cDNA and appropriate promoters for cRNA transcription. Plasmids were linearized before cRNA synthesis, and mMESSAGE MACHINE kits (Ambion) were used to generate capped cRNA. cRNA was injected into oocytes at a volume of 50 nl/oocyte using a Drummond microinjector. Oocytes were maintained in a saline buffer (96 mM NaCl, 2 mM KCl, 1 mM $MgCl_2$, 1 mM $CaCl_2$, and 5 mM HEPES, pH 7.5) solution supplemented with 5% (v/v) heat-inactivated horse serum, sodium pyruvate (2.5 mM), gentamycin (50 μg/ml). A valve system controlled by the data acquisition software pCLAMP 6 (Axon Instruments) was used to control solution changes and to minimize washing and washout times. Two-electrode voltage clamp recordings of the oocytes were performed 36–72 h after cRNA injection. Membrane potential was clamped at −80 mV using a AxoClamp 900A amplifier (Molecular Devices) and pCLAMP 6 software. Electrodes were filled with 3 M KCl and had resistances of 0.5–1.5 megaohms. To reveal inward currents through the inwardly rectifying GIRK channels, recordings were performed in oocyte saline buffer with elevated (16 mM) KCl concentrations (other components were 82 mM NaCl, 1 mM $MgCl_2$, 1 mM $CaCl_2$, and 5 mM HEPES, pH 7.5). After electrophysiological recording, oocytes were sonicated in ice-cold phosphate-buffered saline containing protease inhibitors. 30 μl of phosphate-buffered saline was added per oocyte. The homogenate was centrifuged at 750 × *g* at 4 °C for 10 min, and the resultant supernatant was used as a whole protein extract of oocytes. To compare the expression levels of RGS11 proteins in oocytes, Western blotting of the whole protein extracts was performed using rabbit anti-RGS11 CT antibody.

Curve-fitting and Statistical Analysis—Kinetic analysis and curve-fitting were performed using pCLAMP 6 software. Time constants (τ) were derived from the exponentials fitted to the activation and deactivation phases of the GIRK currents. Cursors were positioned at points on the activation and deactivation curves that corresponded to 20 and 80% of the maximum equilibrium responses, and the exponentials were fitted to the portions of the current trace between these two points. We used Student's *t* test for comparison of the independent means. Two-tailed *p* value <0.01 is defined as significantly different.

RESULTS

R9AP Enhances GAP Activity of RGS11 by a Membrane-delimited Mechanism—Purified uROS have proven to be a valuable model for delineating activity regulation mechanisms of RGS9-1, the closest homologue of RGS11 (34, 35). Because urea treatment removes the G protein transducin (Gα_t) and associated GAPs but leaves endogenous R9AP and GPCR rhodopsin intact (20), we used this preparation as an initial reagent to study the effects of R9AP on the RGS11·Gβ_5 complex. Previous studies have shown that anchoring purified RGS9-1·Gβ_5 by native R9AP contained within the uROS preparation markedly potentiates its GAP activity toward exogenously added Gα_t (19–21). Because Gα_t is not the physiological substrate of the RGS11·Gβ_5 complex (23), we first demonstrated that the uROS system could be exploited to study the effects of R9AP on the GTP hydrolysis catalyzed by Gα_o, a G protein specifically co-expressed with the RGS11 in the ON-bipolar neurons (23, 25, 26). The addition of increasing amounts of RGS9-1·Gβ_5 to the uROS membranes reconstituted with lipid-modified Gα_o, expressed and purified from Sf9 cells, produced a typical biphasic concentration dependence curve with an initial steep slope of 0.09 ± 0.01 $s^{-1}\mu M^{-1}$ catalytic activity rate followed by a shallower slope defined by a specific activity of 0.020 ± 0.003 $s^{-1}\mu M^{-1}$ (Fig. 1*A*). Previous studies have established that the inflection point in the curve corresponds to the concentration of active R9AP on the membranes (20, 21), and therefore, the initial steeper slope is interpreted as the specific activity of the R9AP-bound RGS complex, whereas the second shallower slope reflects the specific activity of excess RGS that remains free after all the R9AP in the reaction mixture has been bound up. Comparison of the two slopes indicates that binding of RGS9-1·Gβ_5 to endogenous R9AP on the membranes can potentiate its GAP activity toward Gα_o by ~5-fold. Consistent with this, we found that RGS9-1·Gβ_5 was efficiently recruited to the uROS membranes and that digestion of R9AP by V8 protease completely abolished association of RGS9-1·Gβ_5 with the V8-treated uROS membranes (V8-uROS) (Fig. 1*B*). Although the magnitude of the stimulatory effect by R9AP is lower than seen in the Gα_t-based system (21), the results clearly indicate that this broken cell preparation can be used to assay the GAP activity of R7 RGS proteins toward Gα_o, making this system amenable for assaying the action of R9AP on the GAP function of RGS11 toward Gα_o.

We found that recombinant RGS11·Gβ_5 was also able to strongly bind to native uROS membranes but not to the

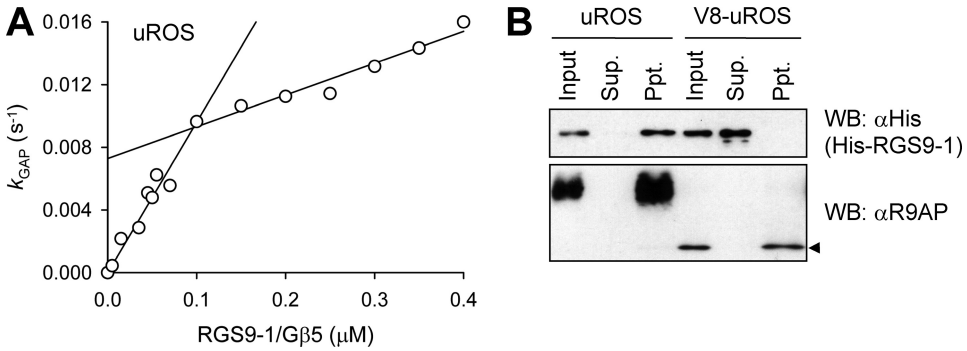

FIGURE 1. **Membrane anchorage of RGS9-1·Gβ_5 by R9AP enhances GAP activity toward Gα_o.** *A*, single-turnover GTPase assay was performed at a fixed concentration of uROS with increasing concentrations of RGS9-1·Gβ_5 as described under "Experimental Procedures." The rate constant of Gα GTPase measured in the absence of RGS proteins (0.023 ± 0.003) was subtracted from the value measured with RGS proteins, and the resulting k_{GAP} values were plotted on the graph. Lipid modified Gα_o purified from Sf9 cells was used. Two independent experiments were conducted, and all of the obtained data are plotted in one graph. *B*, recombinant histidine-tagged RGS9-1 expressed in and purified from Sf9 cells co-expressing Gβ_5 protein was incubated with uROS membranes and analyzed for the ability to co-sediment with the membranes. The presence of RGS9-1 and R9AP protein in the total incubation mixture (*Input*) and the supernatants and membrane pellets produced after centrifugation was determined by Western blotting. The *top* and *bottom panels* in *B* depict Western blots (*WB*) with an anti-histidine tag antibody (*αHis*) and with an anti-R9AP antibody (*αR9AP*), respectively. In the *bottom panel* in *B*, the prominent higher molecular weight bands are full-length R9AP, and an *arrowhead* indicates the degradation products of R9AP (observed only with V8-uROS).

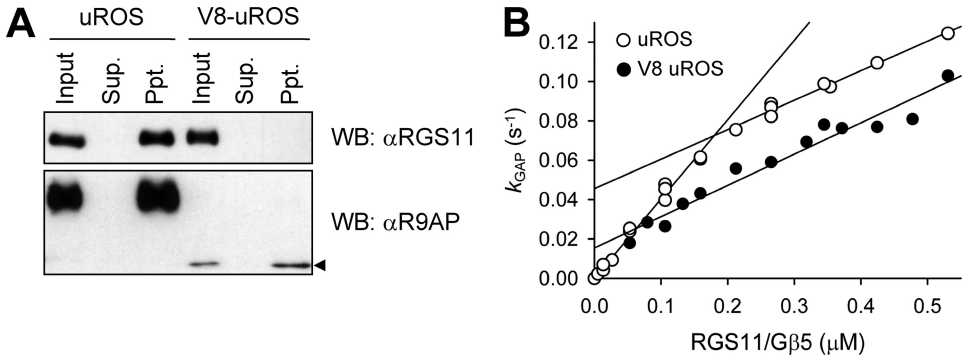

FIGURE 2. **Endogenous R9AP anchors RGS11·Gβ_5 on the membranes and potentiates GAP activity toward lipid-modified Gα_o.** *A*, membrane binding assay was performed with RGS11·Gβ_5 as described in the legend for Fig. 1. *WB*, Western blot. *B*, single-turnover GTPase assays were performed at a fixed concentration of uROS (○) or V8-uROS (●) with increasing concentrations of RGS11·Gβ_5 as described in the legend for Fig. 1. Lipid-modified Gα_o purified from Sf9 cells was used. The rate constants of Gα GTPase measured in the absence of RGS proteins (0.022 ± 0.001 s^{-1} for uROS and 0.019 ± 0.003 s^{-1} for V8 uROS) were subtracted from the values measured with RGS proteins, and the resulting k_{GAP} values were plotted on the graph. Three independent experiments with each membrane preparation were conducted, and all of the obtained data are plotted in one graph.

V8-uROS (Fig. 2*A*). As observed for RGS9-1, GTPase hydrolysis rates of Gα_o showed biphasic dependence on the RGS11·Gβ_5 concentration (Fig. 2*B*, *open circles*), and the biphasic concentration dependence was completely abolished by the V8-mediated proteolysis of R9AP (Fig. 2*B*, *filled circles*). Comparing the specific activity rate of RGS11·Gβ_5 in the fast phase (0.39 ± 0.02 $s^{-1}\mu M^{-1}$) to the slow phase (0.15 ± 0.01 $s^{-1}\mu M^{-1}$) or to the activity in the V8-treated system (0.16 ± 0.01 $s^{-1}\mu M^{-1}$) reveals that R9AP enhances GAP activity of RGS11·Gβ_5 by ~2.5-fold.

Interestingly, when RGS11·Gβ_5 was incubated with V8-uROS and the mixture subsequently fractionated by centrifugation, the RGS11 protein was not detected in either the Sup or Ppt fractions (Fig. 2*A*). The absence of RGS11 in both V8-treated fractions can be explained if the RGS11·Gβ_5 complex can associate directly (*i.e.* independently of R9AP) with the membranes and sediment with the membrane pellet. The association is weak enough, however, to be disrupted by the stringent conditions under which the pellet is washed (see "Experimental Procedures"), resulting in the removal of RGS11·Gβ_5 complex from the membrane pellet. Indeed, skipping the washing steps resulted in a robust detection of RGS11 in a pellet fraction (supplemental Fig. 2). RGS9-1·Gβ_5 is not targeted to the V8-uROS membranes in this manner (*i.e.* without R9AP, see Fig. 1*B*). Consequently, the activity of non-R9AP-bound, RGS11·Gβ_5 (0.16 ± 0.01 $s^{-1}\mu M^{-1}$, shallow slopes in Fig. 2*B*) was substantially higher than that of free RGS9-1·Gβ_5 (0.02 ± 0.003 $s^{-1}\mu M^{-1}$, shallow slope in Fig. 1*A*), suggesting that the activity of RGS11·Gβ_5 can be enhanced by R9AP-independent membrane association that brings it in the vicinity of lipid-modified Gα_o.

To analyze the contribution of such membrane localization to the activity of the RGS11·Gβ_5 complex, the above assay was repeated with a soluble Gα_o that was unable to tightly associate with the uROS membranes (Fig. 3*A*). This preparation of Gα_o was obtained by expression in *E. coli* known to produce protein devoid of posttranslational lipid modifications (40). The Gα_o purified from *E. coli* showed intrinsic GTPase activity (k_{app} = 0.021 ± 0.005 s^{-1}) similar to that of the lipid-modified Gα_o from Sf9 cells (k_{app} = 0.027 ± 0.007 s^{-1}) that was effectively accelerated by the addition of soluble RGS proteins (*e.g.* RGS7, supplemental Fig. 1). However, the RGS11·Gβ_5 GAP activity targeted to the soluble non-lipid-modified Gα_o from *E. coli* was not biphasic. The entire activity *versus* concentration plot (Fig. 3*B*) could be fitted with a single shallow slope characterized by a catalytic rate of only 0.043 ± 0.003 $s^{-1}\mu M^{-1}$. This rate is closer to the GAP rate displayed by the non-R9AP-bound form of RGS9-1·Gβ_5 (0.02 ± 0.003 $s^{-1}\mu M^{-1}$), which does not exhibit intrinsic membrane binding (Fig. 1*B*).

The role of membrane anchoring by R9AP in activity regulation of RGS11·Gβ_5 was further delineated using an R9AP deletion mutant rendered soluble by deleting a transmembrane region (R9APΔTM). Incubation with this construct prevented association of RGS11·Gβ_5 with the uROS membranes, and the RGS11·Gβ_5 complex remained in the supernatant after centrifugation of the reaction mixture (Fig. 4*A*). Concurrently, R9APΔTM also dramatically reduced the GAP activity of RGS11 (Fig. 4*B*). At the same time, R9APΔTM did not have any

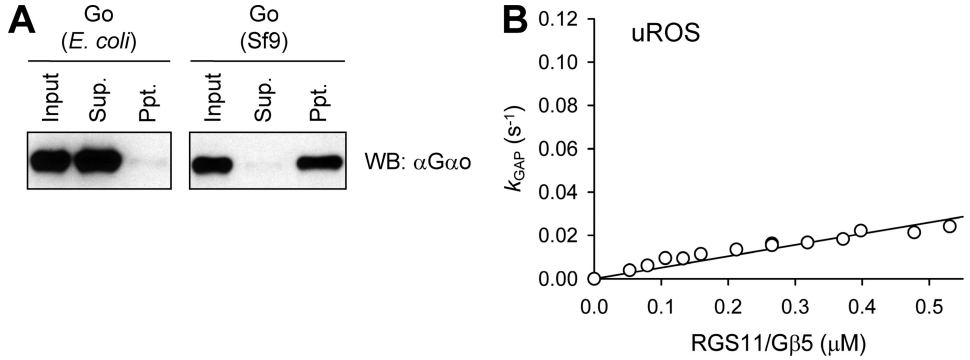

FIGURE 3. **Membrane anchoring of RGS11·Gβ_5 does not change GAP activity toward soluble Gα_o.** *A*, membrane binding activity of Gα_o purified from *E. coli* or Sf9 cells were tested by incubating Gα_o with uROS membranes, and Western blotting (*WB*) was performed with anti-Gα_o antibody (α-Gα_o). *B*, a single-turnover GTPase assay was performed at a fixed concentration of uROS with increasing concentrations of RGS11·Gβ_5 as described in the legend of Fig. 1 but with soluble Gα_o purified from *E. coli*. The rate constant of Gα GTPase measured in the absence of RGS proteins (0.020 ± 0.003 s^{-1}) was subtracted from the value measured with RGS proteins, and the resulting k_{GAP} values are plotted on the graph. Two independent experiments with each membrane preparation were conducted, and all of the obtained data are plotted in one graph.

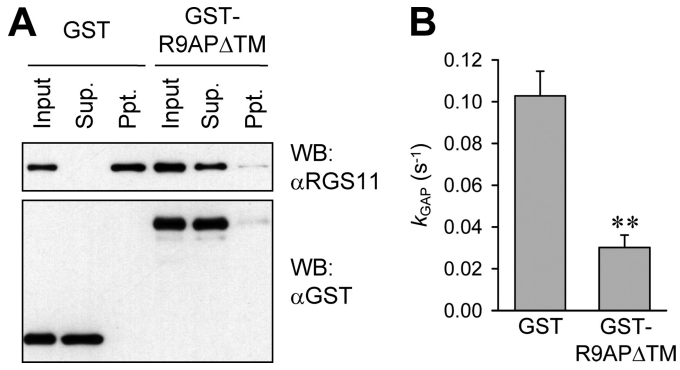

FIGURE 4. **Inhibition of RGS11·Gβ_5 GAP activity by dominant-negative soluble R9AP mutant.** *A*, membrane binding was assayed by incubating RGS11·Gβ_5 with uROS membranes in the presence of GST or GST-R9APΔTM and Input, Sup, and Ppt fractions were probed by Western blotting with anti-RGS11 antibodies (αRGS11; *upper panel*). The solubilities of GST and the GST-R9APΔTM proteins were evaluated by probing Input, Sup, and Ppt fractions with an anti-GST antibodies (αGST; *lower panel*). *WB*, Western blot. *B*, GAP activity of RGS11·Gβ_5 was measured in the presence of GST or a GST fusion of the soluble R9AP mutant (GST-R9APΔTM) by single-turnover GTPase assay using a fixed concentration of RGS11·Gβ_5 and lipid-modified Gα_o. The concentration of RGS11·Gβ_5 at the inflection point (180 nM) in Fig. 1*C* was chosen, and data are expressed as the means ± S.E. from three independent experiments. **, $p < 0.01$ (unpaired *t* test).

effect on the Gα_o GTPase activity in the absence of RGS11·Gβ_5 (supplemental Fig. 3). These observations indicate that membrane anchoring of RGS11·Gβ_5 enhances its GAP activity by localizing it in close proximity to Gα_o.

To further prove that R9AP mediates the potentiation of RGS11·Gβ_5 GAP function, we have performed a reconstitution experiment. For this, membranes prepared from Sf9 insect cells expressing recombinant R9AP were added in *trans* to the V8-uROS membranes. Data shown in Fig. 5*A* demonstrate that the addition of the R9AP-expressing Sf9 membranes partitions recombinant RGS11·Gβ_5 away from the soluble fraction to the particulate fraction and increases its activity by ~2-fold, resulting in nearly complete restoration of RGS11 activity lost upon the V8 treatment of the uROS membranes (~2.5 times; Fig. 5*B*). At the same time, R9AP-containing Sf9 membranes did not change the basal rates of Gα_o GTPase activity (supplemental Fig. 4). Taken together, these findings indicate that specific anchoring by R9AP potentiates the activity of RGS11·Gβ_5 via a membrane-delimited mechanism.

R9AP Augments Regulatory Activity of RGS11 on mGluR6-Gα_o Signaling in Xenopus Oocytes—Recent studies suggest that RGS11·Gβ_5·R9AP complex acts as a GAP for Gα_o in retinal ON-bipolar neurons where it is selectively recruited to mGluR6, a G protein-coupled receptor that is thought to activate the Gα_o when the neurons respond to glutamate released from the photoreceptors (23–25). Therefore, we have next sought to determine the effect of the R9AP on RGS11 GAP function at a cellular level in the context of this physiologically relevant receptor, mGluR6, and the cognate G protein, Gα_o. We have reconstituted coupling between mGluR6 and Gα_o using a well established *Xenopus* oocytes expression system and utilized co-expressed GIRK channels to study the kinetics of the physiologically relevant coupling between mGluR6 and Gα_o. The kinetics of the channel deactivation depend crucially on the rate at which the free G$\beta\gamma$ is re-sequestered by inactive Gα, which in turn depends on GTPase activity of the Gα. Thus, the acceleration of the GIRK channel deactivation rate by co-expressed RGS proteins provides a convenient measure of the GAP function of RGS protein in live cells that has with the high sensitivity and temporal resolution (for review, see Ref. 37). The contribution of endogenous *Xenopus* G proteins to our kinetic measures was eliminated by co-expressing the catalytic subunit of pertussis toxin (PTX) and by utilizing a pertussis toxin insensitive Gα_o construct, Gα_oC351A. Consistent with an earlier report (41), heterologous expression of mGluR6, PTX catalytic subunit, PTX-insensitive Gα_oC351A, and GIRK1/GIRK4 subunits allowed for the detection of inward currents through the GIRK channels (downward and upward deflections in current traces depicted in Fig. 6*A*) in response to mGluR6 stimulation by glutamate application and extinction upon glutamate washout (shown in *black* in Fig. 6, *A* and *B*). No glutamate-elicited currents were observed when the PTX catalytic subunit was expressed in the absence of the PTX-insensitive Gα_oC351A G protein subunit (data not shown). The injection of oocytes with cRNA for RGS11 and Gβ_5 (2 ng each) did not have any significant effect on the kinetics of the response (*blue versus black traces in* Fig. 6, *A* and *B*) despite robust expression of RGS11·Gβ_5 in cells (Fig. 6*C*). However, co-expression of RGS11·Gβ_5 with R9AP dramatically accelerated both the activation and deactivation kinetics of glutamate-evoked GIRK currents (shown in *red* in Fig. 6, *A* and *B*), which are the hallmarks of GIRK channel modulation by the GAP activity of RGS proteins (38, 39, 42, 43). The apparent acceleration of the activation kinetics are in fact an unsurprising and necessary consequence of the accelerated deactivation kinetics; for most reversible reactions the time

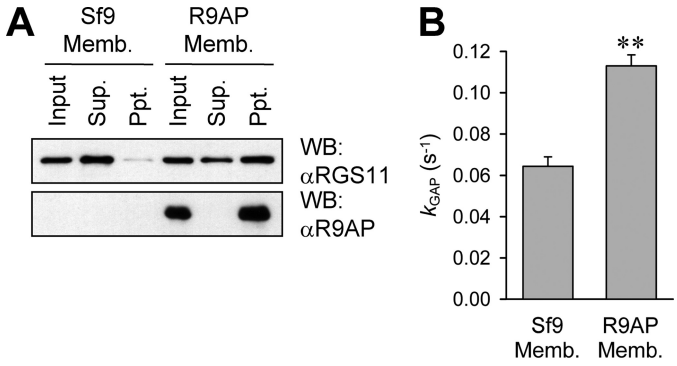

FIGURE 5. **Membrane-bound recombinant R9AP potentiates GAP activity of RGS11·Gβ_5.** *A*, membrane binding was assayed by incubating RGS11·Gβ_5 with either Sf9 membranes or Sf9 membranes, expressing recombinant R9AP (*R9AP Memb.*) and Input, Sup, and Ppt fractions were probed by Western blotting with anti-RGS11 antibodies (αRGS11; *upper panel*). The expression of R9AP in the membranes prepared from the Sf9 cells was evaluated by probing Input, Sup, and Ppt fractions with anti-R9AP antibodies (αR9AP; *lower panel*). *WB*, Western blot. *B*, effects of control Sf9 membranes (*Sf9 Memb.*) or Sf9 membranes expressing recombinant R9AP (*R9AP Memb.*) on GAP activity of RGS11·Gβ_5 (180 nM) were examined. GAP activity was measured by a single-turnover GTPase assay using lipid-modified Gα_o and V8-uROS. Data are expressed as the means ± S.E. from three independent experiments. **, $p <$ 0.01 (unpaired *t* test).

required to reach equilibrium (*i.e.* the peak GIRK current amplitude) after the forward reaction is set in motion is shortened when either the forward or the backward rate of the reaction (deactivation rate) is increased (see Ref. 39 for a comprehensive account). Note that the averaged activation and deactivation traces depicted in Fig. 6*A* have been normalized against the peak level of GIRK current. The normalization was performed so that the altered kinetics depicted by the traces can be compared appropriately. Expression of R9AP alone (*i.e.* in the absence of RGS11·Gβ_5) had no effect on GIRK kinetics (data not shown), indicating that the stimulatory effect of R9AP is mediated through RGS11·Gβ_5. Comparison of the protein expression by Western blotting showed a modest increase in RGS11 levels upon co-expression with R9AP (Fig. 6*C*), consistent with the role of R9AP in protecting RGS11·Gβ_5 from rapid proteolytic degradation (23). However, this rather modest increase in RGS11·Gβ_5 levels (not exceeding 2-fold) cannot explain an all-or-nothing effect of R9AP addition on the ability of RGS11·Gβ_5 to accelerate activation and deactivation kinetics. In summary, these observations indicate that R9AP is necessary for the GAP function of RGS11·Gβ_5 protein complex on mGluR6-Gα_o signaling in a cell-based system.

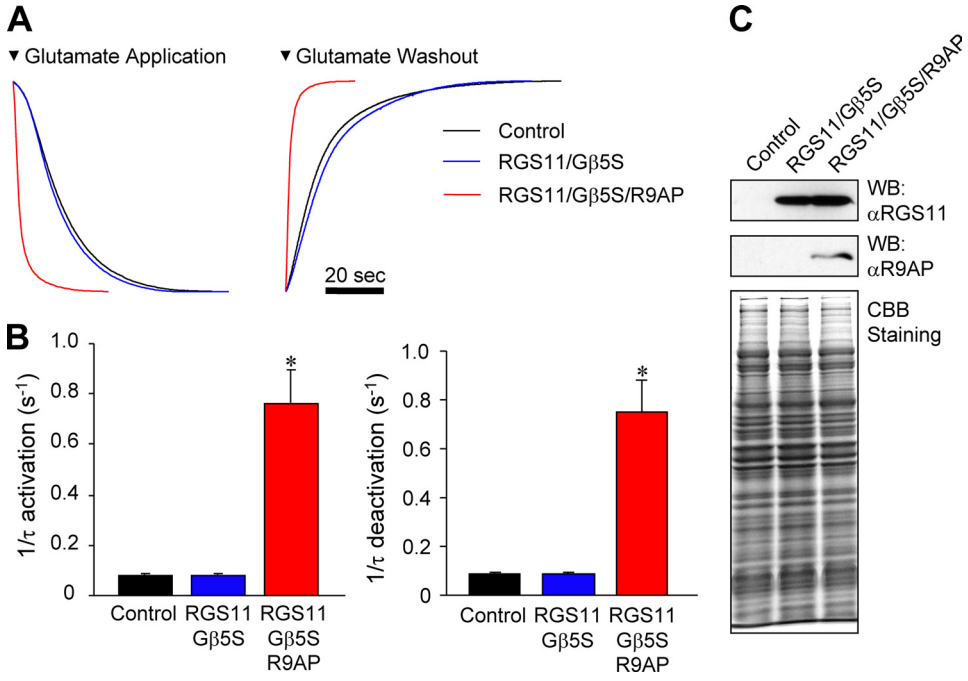

FIGURE 6. **Association with R9AP is essential for RGS11·Gβ_5-mediated regulation of mGluR6-Gα_o signaling in *Xenopus* oocytes.** Control oocytes were injected with cRNAs for mGluR6, Gα_oC351G, and GIRK1 and GIRK4 subunits of heteromultimeric GIRK channels and with cRNA for the catalytic subunit of pertussis toxin to eliminate coupling between mGluR6 and endogenous $G_{i/o}$ G proteins. Some of these control oocytes were subsequently injected with either water or one of the following cRNA combinations in addition to those described above: (i) RGS11 and Gβ_5 or (ii) RGS11, Gβ_5, and R9AP. *A*, normalized averaged traces of glutamate (10 μM) evoked GIRK currents. The figure shows activation (downward deflection, *left*) and deactivation (upward deflection, *right*) phases of the glutamate-evoked GIRK currents in the three oocyte groups. *B*, a comparison is shown of the activation and deactivation rate constants ($1/\tau$), where τ is the time constant derived from the exponential fits of the activation and deactivation phases of the GIRK currents in the different oocyte groups. Data are expressed as the means ± S.E. from 7–9 oocytes from the same donor. The mean steady-state current amplitudes in nA ± S.E. for the different oocyte groups were as follows: control, 941 ± 37; RGS11·Gβ_5, 1024 ± 255; RGS11·Gβ_5·R9AP, 658 ± 76. Similar results were obtained from multiple oocyte donors. *, significantly different from control ($p < 0.05$ by Student's *t* test). *WB*, Western blot. *C*, whole protein extracts were prepared from oocytes after electrophysiological recording and expression levels of RGS11 and R9AP were analyzed by Western blotting with specific antibodies or by Coomassie Brilliant Blue (*CBB*) staining.

DISCUSSION

The main conclusion from our study is that R9AP positively modulates the GAP activity of RGS11·Gβ_5 complex *in vitro* and is essential for the ability of the RGS11 complex to regulate mGluR6 signaling in cells. In addition, we show that R9AP-mediated acceleration of the GAP activity is not confined to the RGS9-transucin system but is likely to be a more universal mechanism of R9AP action. The stimulatory effect of R9AP requires that it is localized at the membrane with the α subunits of the G proteins. Disruption of this co-localization by either dominant negative soluble R9AP or by the use of non-lipid-modified Gα_o abolished potentiation by R9AP, indicating the critical contribution of membrane association to the action of R9AP. These observations also suggest that changes in lipid modification status of Gα_o (for review, see Ref. 22) would have profound consequences on the acceleration of inactivation by some R7 RGS family members. More specifically, the duration of Gα_o signaling in the mGluR6 cascade of ON-bipolar cells is expected to be substantially influenced by dynamics of palmitoylation and/or myristoylation of Gα_o.

Results of this study suggest that the stimulatory effect of R9AP toward the RGS11·Gβ_5 complex involves an allosteric enhancement of GAP function acting in addition to the potentiation produced by membrane recruitment (see supplemental Fig. 5 for a schematic illustration). First, we found that RGS11·Gβ_5 has an intrinsic propensity to associate directly and independently of R9AP with the uROS membranes, a broken photoreceptor cell preparation. However, recruitment of RGS11·Gβ_5 to the same membranes by R9AP produces greater potentiation of its GAP activity that cannot be simply explained by the concentration of the complex at the membrane. Furthermore, in a cellular system reconstituted with the physiologically relevant receptor, mGluR6, RGS11·Gβ_5 did not detectably accelerate the GTPase activity of the mGluR6-coupled G protein Gα_o unless R9AP was co-expressed and conferred strong GAP activity to the RGS11·Gβ_5 complex. Interestingly, the R9AP-mediated enhancement of RGS11·Gβ_5 GAP function at Gα_o coupled to rhodopsin in the uROS system was only ~2.5-fold. This observation suggests that the stimulatory effects of R9AP exhibit GPCR selectivity and, cannot be solely explained by membrane recruitment. Finally, comparing the activity of the RGS9-1·Gβ_5 complex in the same rhodopsin-based system reveals that despite equal membrane recruitment, R9AP has much greater stimulatory effect toward Gα_t (~70-fold; Ref. 21) as compared with Gα_o (~5-fold; this study). Taken together, these observations indicate that the allosteric effects of R9AP at the R7 RGS proteins might in fact contribute to the G protein and GPCR selectivity of the R7 RGS proteins. In summary, our study establishes R9AP as a subunit of R7 RGS complexes with a general function of GAP activity modulator that acts by allosteric mechanisms in addition to membrane recruitment.

Acknowledgments—We thanks to Hideko Masuho for technical assistance and Garret Anderson for the purification of GST-R9APΔTM protein.

REFERENCES

1. Hollinger, S., and Hepler, J. R. (2002) *Pharmacol. Rev.* **54,** 527–559
2. Ross, E. M., and Wilkie, T. M. (2000) *Annu. Rev. Biochem.* **69,** 795–827
3. Garzón, J., López-Fando, A., and Sánchez-Blázquez, P. (2003) *Neuropsychopharmacology* **28,** 1983–1990
4. Nishiguchi, K. M., Sandberg, M. A., Kooijman, A. C., Martemyanov, K. A., Pott, J. W., Hagstrom, S. A., Arshavsky, V. Y., Berson, E. L., and Dryja, T. P. (2004) *Nature* **427,** 75–78
5. Rahman, Z., Schwarz, J., Gold, S. J., Zachariou, V., Wein, M. N., Choi, K. H., Kovoor, A., Chen, C. K., DiLeone, R. J., Schwarz, S. C., Selley, D. E., Sim-Selley, L. J., Barrot, M., Luedtke, R. R., Self, D., Neve, R. L., Lester, H. A., Simon, M. I., and Nestler, E. J. (2003) *Neuron* **38,** 941–952
6. Zachariou, V., Georgescu, D., Sanchez, N., Rahman, Z., DiLeone, R., Berton, O., Neve, R. L., Sim-Selley, L. J., Selley, D. E., Gold, S. J., and Nestler, E. J. (2003) *Proc. Natl. Acad. Sci. U.S.A.* **100,** 13656–13661
7. Anderson, G. R., Posokhova, E., and Martemyanov, K. A. (2009) *Cell Biochem. Biophys.* **54,** 33–46
8. Snow, B. E., Krumins, A. M., Brothers, G. M., Lee, S. F., Wall, M. A., Chung, S., Mangion, J., Arya, S., Gilman, A. G., and Siderovski, D. P. (1998) *Proc. Natl. Acad. Sci. U.S.A.* **95,** 13307–13312
9. Martemyanov, K. A., Yoo, P. J., Skiba, N. P., and Arshavsky, V. Y. (2005) *J. Biol. Chem.* **280,** 5133–5136
10. Hu, G., Zhang, Z., and Wensel, T. G. (2003) *J. Biol. Chem.* **278,** 14550–14554
11. Witherow, D. S., Wang, Q., Levay, K., Cabrera, J. L., Chen, J., Willars, G. B., and Slepak, V. Z. (2000) *J. Biol. Chem.* **275,** 24872–24880
12. Chen, C. K., Eversole-Cire, P., Zhang, H., Mancino, V., Chen, Y. J., He, W., Wensel, T. G., and Simon, M. I. (2003) *Proc. Natl. Acad. Sci. U.S.A.* **100,** 6604–6609
13. Anderson, G. R., Semenov, A., Song, J. H., and Martemyanov, K. A. (2007) *J. Biol. Chem.* **282,** 4772–4781
14. Keresztes, G., Martemyanov, K. A., Krispel, C. M., Mutai, H., Yoo, P. J., Maison, S. F., Burns, M. E., Arshavsky, V. Y., and Heller, S. (2004) *J. Biol. Chem.* **279,** 1581–1584
15. Krispel, C. M., Chen, D., Melling, N., Chen, Y. J., Martemyanov, K. A., Quillinan, N., Arshavsky, V. Y., Wensel, T. G., Chen, C. K., and Burns, M. E. (2006) *Neuron* **51,** 409–416
16. Song, J. H., Waataja, J. J., and Martemyanov, K. A. (2006) *J. Biol. Chem.* **281,** 15361–15369
17. Drenan, R. M., Doupnik, C. A., Boyle, M. P., Muglia, L. J., Huettner, J. E., Linder, M. E., and Blumer, K. J. (2005) *J. Cell Biol.* **169,** 623–633
18. Hu, G., and Wensel, T. G. (2002) *Proc. Natl. Acad. Sci. U.S.A.* **99,** 9755–9760
19. Baker, S. A., Martemyanov, K. A., Shavkunov, A. S., and Arshavsky, V. Y. (2006) *Biochemistry* **45,** 10690–10697
20. Lishko, P. V., Martemyanov, K. A., Hopp, J. A., and Arshavsky, V. Y. (2002) *J. Biol. Chem.* **277,** 24376–24381
21. Martemyanov, K. A., Lishko, P. V., Calero, N., Keresztes, G., Sokolov, M., Strissel, K. J., Leskov, I. B., Hopp, J. A., Kolesnikov, A. V., Chen, C. K., Lem, J., Heller, S., Burns, M. E., and Arshavsky, V. Y. (2003) *J. Neurosci.* **23,** 10175–10181
22. Chen, C. A., and Manning, D. R. (2001) *Oncogene* **20,** 1643–1652
23. Cao, Y., Masuho, I., Okawa, H., Xie, K., Asami, J., Kammermeier, P. J., Maddox, D. M., Furukawa, T., Inoue, T., Sampath, A. P., and Martemyanov, K. A. (2009) *J. Neurosci.* **29,** 9301–9313
24. Mojumder, D. K., Qian, Y., and Wensel, T. G. (2009) *J. Neurosci.* **29,** 7753–7765
25. Morgans, C. W., Wensel, T. G., Brown, R. L., Perez-Leon, J. A., Bearnot, B., and Duvoisin, R. M. (2007) *Eur. J. Neurosci.* **26,** 2899–2905
26. Rao, A., Dallman, R., Henderson, S., and Chen, C. K. (2007) *J. Neurosci.* **27,** 14199–14204
27. Vardi, N., Dhingra, A., Zhang, L., Lyubarsky, A., Wang, T. L., and Morigiwa, K. (2002) *Keio J. Med.* **51,** 154–164
28. Keresztes, G., Mutai, H., Hibino, H., Hudspeth, A. J., and Heller, S. (2003) *Mol. Cell. Neurosci.* **24,** 687–695
29. Cao, Y., Song, H., Okawa, H., Sampath, A. P., Sokolov, M., and Martemyanov, K. A. (2008) *J. Neurosci.* **28,** 10443–10449
30. Song, J. H., Song, H., Wensel, T. G., Sokolov, M., and Martemyanov, K. A. (2007) *Mol. Cell. Neurosci.* **35,** 311–319
31. Skiba, N. P., Martemyanov, K. A., Elfenbein, A., Hopp, J. A., Bohm, A., Simonds, W. F., and Arshavsky, V. Y. (2001) *J. Biol. Chem.* **276,** 37365–37372
32. Martemyanov, K. A., Hopp, J. A., and Arshavsky, V. Y. (2003) *Neuron* **38,** 857–862
33. Kozasa, T., and Gilman, A. G. (1995) *J. Biol. Chem.* **270,** 1734–1741
34. Martemyanov, K. A., and Arshavsky, V. Y. (2004) *Methods Enzymol.* **390,** 196–209
35. Cowan, C. W., Wensel, T. G., and Arshavsky, V. Y. (2000) *Methods Enzymol.* **315,** 524–538
36. Otto-Bruc, A., Antonny, B., Vuong, T. M., Chardin, P., and Chabre, M. (1993) *Biochemistry* **32,** 8636–8645
37. Doupnik, C. A., Jaén, C., and Zhang, Q. (2004) *Methods Enzymol.* **389,** 131–154
38. Chuang, H. H., Yu, M., Jan, Y. N., and Jan, L. Y. (1998) *Proc. Natl. Acad. Sci. U.S.A.* **95,** 11727–11732
39. Zhong, H., Wade, S. M., Woolf, P. J., Linderman, J. J., Traynor, J. R., and Neubig, R. R. (2003) *J. Biol. Chem.* **278,** 7278–7284
40. Lee, E., Linder, M. E., and Gilman, A. G. (1994) *Methods Enzymol.* **237,** 146–164
41. Dhingra, A., Faurobert, E., Dascal, N., Sterling, P., and Vardi, N. (2004) *J. Neurosci.* **24,** 5684–5693
42. Doupnik, C. A., Davidson, N., Lester, H. A., and Kofuji, P. (1997) *Proc. Natl. Acad. Sci. U.S.A.* **94,** 10461–10466
43. Saitoh, O., Kubo, Y., Miyatani, Y., Asano, T., and Nakata, H. (1997) *Nature* **390,** 525–529

Membrane Anchor R9AP Potentiates GTPase-accelerating Protein Activity of RGS11·Gβ_5 Complex and Accelerates Inactivation of the mGluR6-G_o Signaling

Ikuo Masuho, Jeremy Celver, Abraham Kovoor and Kirill A. Martemyanov

J. Biol. Chem. 2010, 285:4781-4787.
doi: 10.1074/jbc.M109.058511 originally published online December 11, 2009

SUPPLEMENTAL FIGURE LEGENDS

Supplemental Fig. 1. GTP hydrolysis rates of Gαo in the absence or presence of RGS7. *A*: Single turnover GTPase assay was performed as described under "Experimental Procedures" to measure GTPase activity of Go proteins purified from *E. coli* or Sf9 cells in the absence or presence of RGS7. RGS7 was chosen in control experiments due to its potent catalytic activity, solubility and inability to interact with R9AP. Reaction time courses were fitted with single exponents to derive the apparent rate constants (k_{app}) plotted in panel ***B***. Both Go proteins show similar k_{app}, indicating functional Go proteins in both preparations are comparable. In the presence of RGS7 (1 μM for Go (*E. coli*) and 5 μM for Go (Sf9)), Gαo purified from *E. coli* and Sf9 cells shows high k_{app}, 0.27 ± 0.05 and 0.39 ± 0.01 respectively, setting ceiling values for the rates under which GDP/GTP exchange is not limiting the GTP hydrolysis. All rate constants measured in this study are substantially slower than the ceiling values obtained with saturating RGS7 concentration.

Supplemental Fig. 2. RGS11 binds weakly to V8-uROS membranes. Membrane binding assay was performed as described under "Experimental Procedures" except that washing steps were skipped. The data shows that a significant amount of RGS11/Gβ5 was present in membrane pellets (Ppt.), which can be eliminated by washing with 1 M NaCl (see Fig. 2*B*), indicating RGS11/Gβ5 weakly associates with V8-uROS membranes in the absence of R9AP.

Supplemental Fig. 3. Effects of soluble R9AP mutant R9APΔTM on the intrinsic and RGS11/Gβ5-stimulated GTPase activity of lipid-modified Gαo. A: Single turnover GTPase assays were performed with uROS membranes containing endogenous membrane-bound R9AP. Addition of excess amount of soluble GST-R9APΔTM (○) did not affect the intrinsic GTPase activity of Gαo (Sf9) compared to the control experiment with GST (●). However, in the presence of RGS11/Gβ5, GST-R9APΔTM (▽) but not GST (▼) markedly inhibited stimulated GTPase activity. Reaction time courses were fitted with single exponents to derive the apparent rate constants (k_{app}) plotted in panel ***B***

Supplemental Fig. 4. Effects of Sf9 membranes containing recombinant R9AP on RGS11/Gβ5 GAP activity. A: Single turnover GTPase assay with lipid-modified Gαo (Sf9) was conducted with V8-uROS membranes, which lack endogenous R9AP. Intrinsic GTPase activity of Gαo in the absence of RGS11/Gβ5 were indistinguishable when either Sf9 cell membrane expressing R9AP (R9AP Memb.; ○) or membranes from non-infected Sf9 cells (Sf9 Memb.; ●) were added. However, when the reaction was supplemented with RGS11/Gβ5, GTPase activity was higher with the addition of the R9AP-containing Sf9 membranes (△) than with membranes from non-infected Sf9 cells (▲).Reaction time courses were fitted with single exponents to derive the apparent rate constants (k_{app}) plotted in panel ***B***

Supplemental Fig. 5. Membrane targeting and allosteric interactions contribute to regulation of RGS11/Gβ5 activity by R9AP. A: RGS11/Gβ5 is weakly associated with the membranes where it can stimulate the GTP hydrolysis on the lipid-modified Gαo. Dissociation of Gαo from the membrane disrupts their spatial co-localization and prevents efficient stimulation of Gαo GTPase by RGS11/Gβ5 complex. **B:** Interaction of RGS11/Gβ5 with R9AP strengthens membrane association and triggers conformational changes that result in stimulation of RGS11/Gβ5 GAP activity.

Supplemental Figure 1

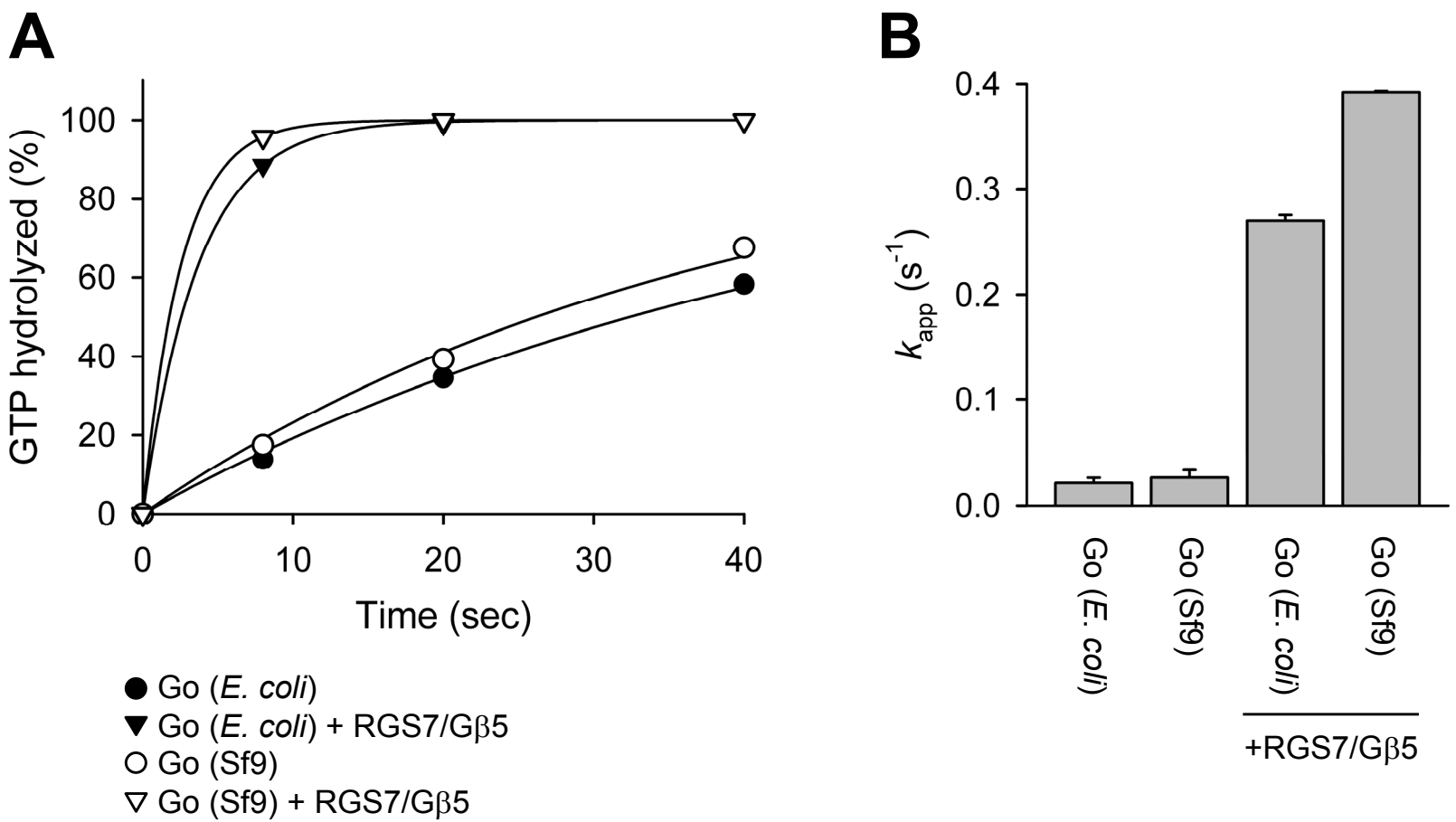

Supplemental Figure 2

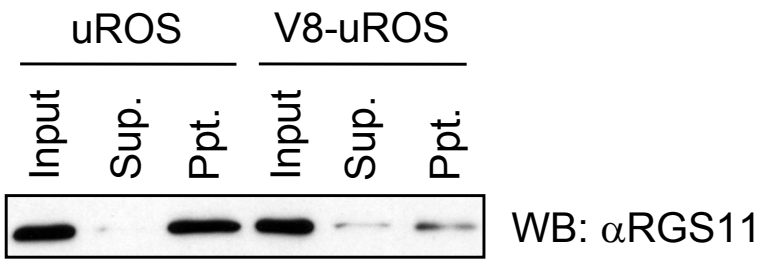

Supplemental Figure 3

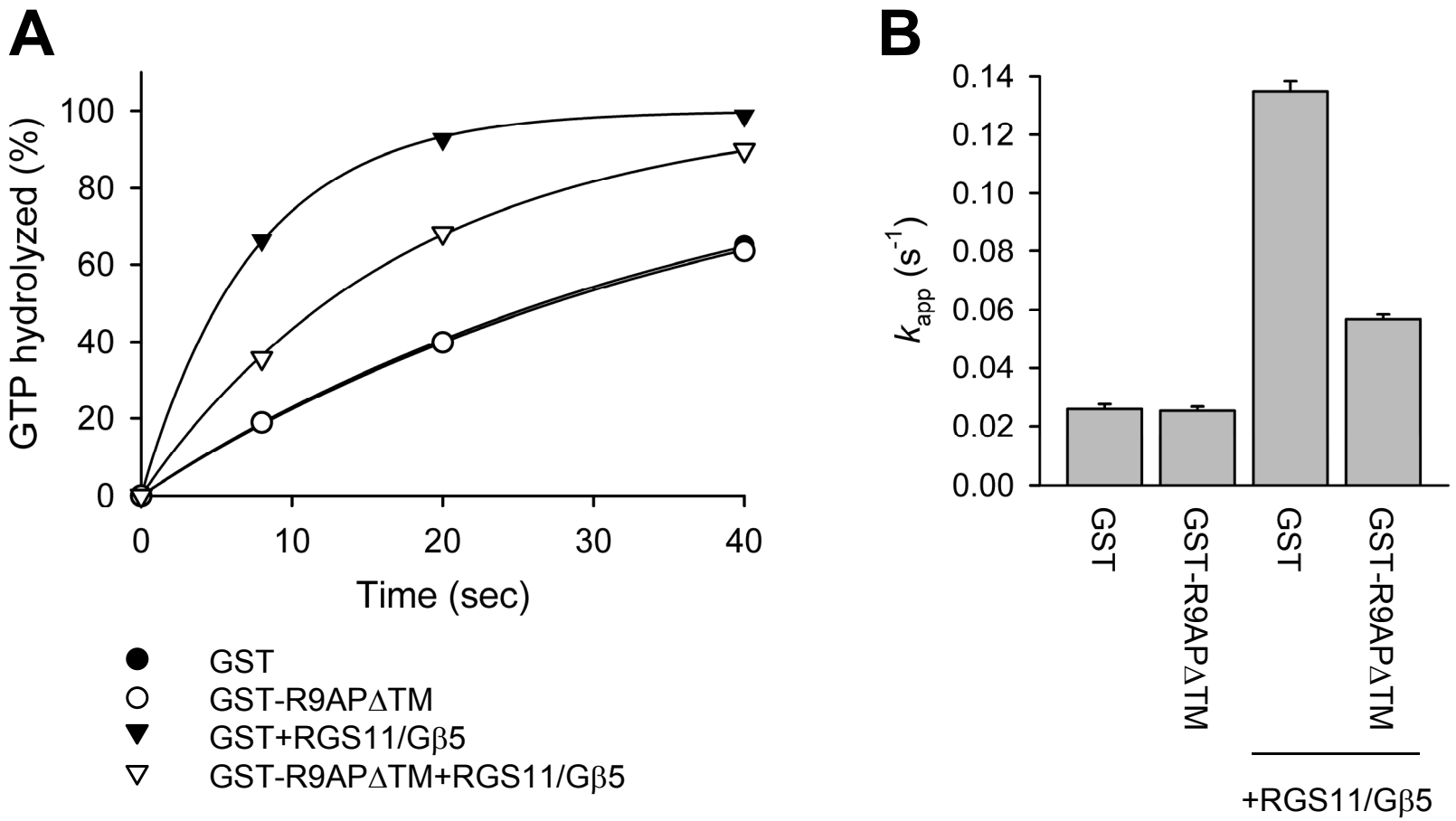

Supplemental Figure 4

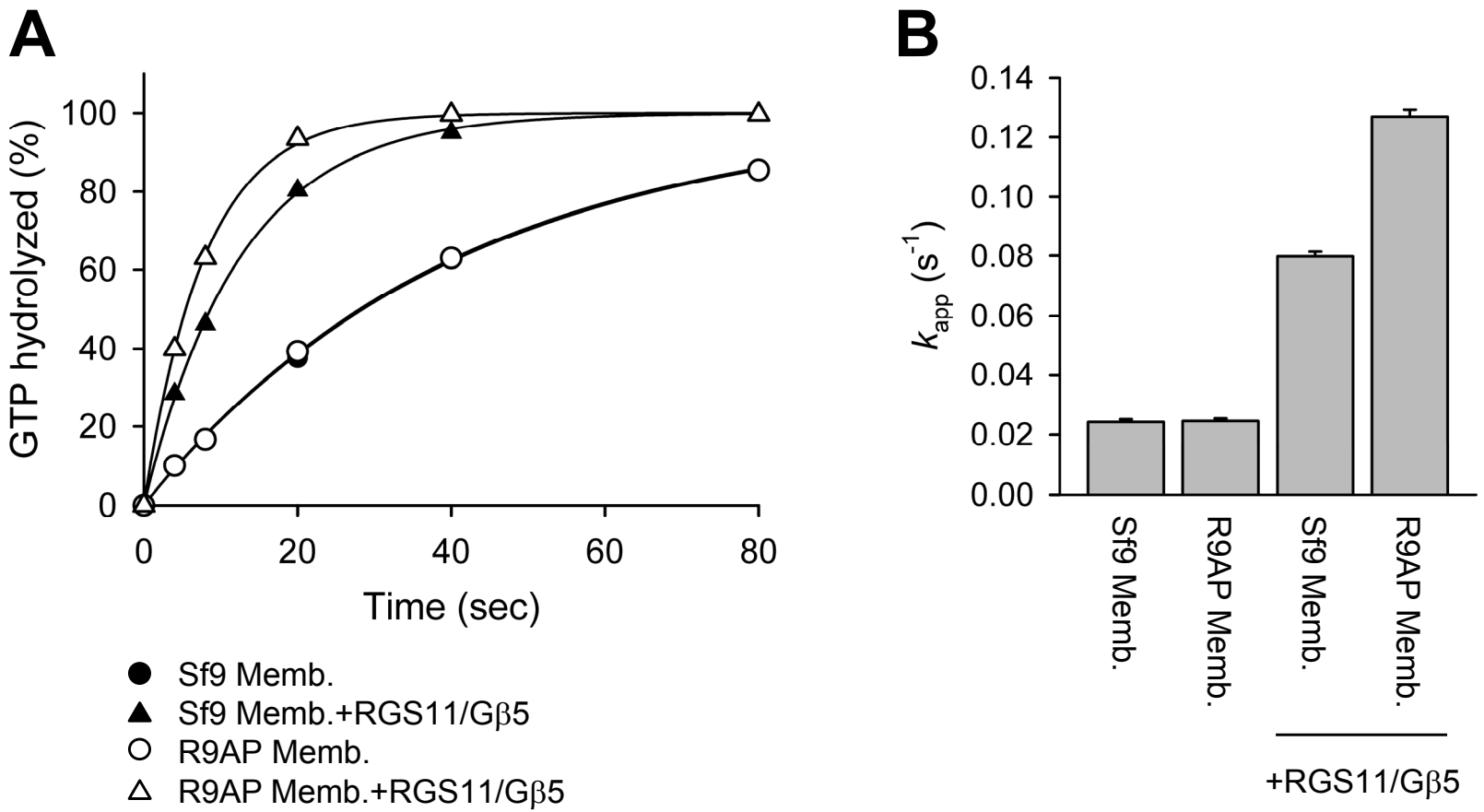

Supplemental Figure 5